3.5   SCCMS Projects

Creatin of material maps by KKR Green's function method

Tetsuya FUKUSHIMA

CD-FMat, National Institute of Advanced Industrial Science and Technology (AIST)

1-1-1 Umezono, Tsukuba, Ibaraki 305-8568, Japan

The purpose of Data Creation and Utilization-Type Material Research and Development Project (Digital Transformation Initiative Center for Magnetic Materials) is to find new functional permanent magnets, soft magnets and spintronics materials by data-driven approaches. The project has placed a high priority on creating materials maps to accelerate the magnetic material developments.

In this year, we generated the magnetic property data, such as magnetization, Curie temperature, and magnetic anisotropy, in preparation for creating the material maps for 1-5 permanent magnets materials[1]. The target materials are $CeCo_5$ alloy series, where the Ce and Co atoms are replaced by the La and Co atoms, respectively. Our calculation is based on the all-electron full-potential Korringa-Kohn-Rostoker (KKR) Green's function method. The randomness of the atomic arrangement is considered by the coherent potential approximation. The spin-orbit coupling is included as the $l_z s_z$ term. The generalized gradient approximation (GGA) is used for the exchange-correlation potential. The space group of the crystal structure is $P6/mmm$, and the lattice constants of the disordered systems are determined by the Vegard rule; the lattice constants of the endpoints is optimized by the full-potential KKR method.

Figure 1 shows the calculated (a) magnetic anisotropy (K_u), (b) magnetization (M_s), (c) anisotropic field ($\mu_0 H_a$), and (d) formation en- ergy (E_{form}) for $Ce_{1-\alpha}La_\alpha Co_{5-x}Fe_x$. K_u is enhanced with a small amount of the Fe atoms and then is gradually decreased with the Fe atoms. The maximum value of K_u is around $x = 0.3$. M_s increases monotonically with the Fe concentration. Therefore, $CeCo_{4.7}Fe_{0.3}$, which has larger K_u and M_s compared to those of $CeCo_5$, is a candidate for new functional permanent magnets. Anisotropic magnetic field is defined by $H_a = \sqrt{2Ku/\mu_0 M_s}$. In the region of $x < 0.3$ for $CeCo_{5-x}Fe_x$, since both K_u and M_s are increased, the change of H_a is small. The formation energy is increased with the Fe concentration, leading to the instability of the 1-5 phase. However, $CeCo_{4.7}Fe_{0.3}$ has still negative formation energy, $E_{from} = -0.19$ eV/f.u., and may stabilize the 1-5 phase.

Next, we consider the effect of the La doping. K_u is decreased monotonically with the La concentration, while M_s is increased. This is due to the hybridization between the Ce-$4f$ and the transition metal $3d$ states, which leads to the enhancement of the occupied electrons in the minority spin states. As a result, the total magnetic moment is decreased. This mechanism is less likely to occur in the La case with the unoccupied $4f$ states. Therefore, the total magnetic moment is expected to be increased when Ce is replaced by La.

The Curie temperature (T_C) of $CeCo_5$ estimated by the full-potential KKR calculations and mean-field approximation is 965 K, which is higher than the experimental value of 653 K. This overestimation is a general error of
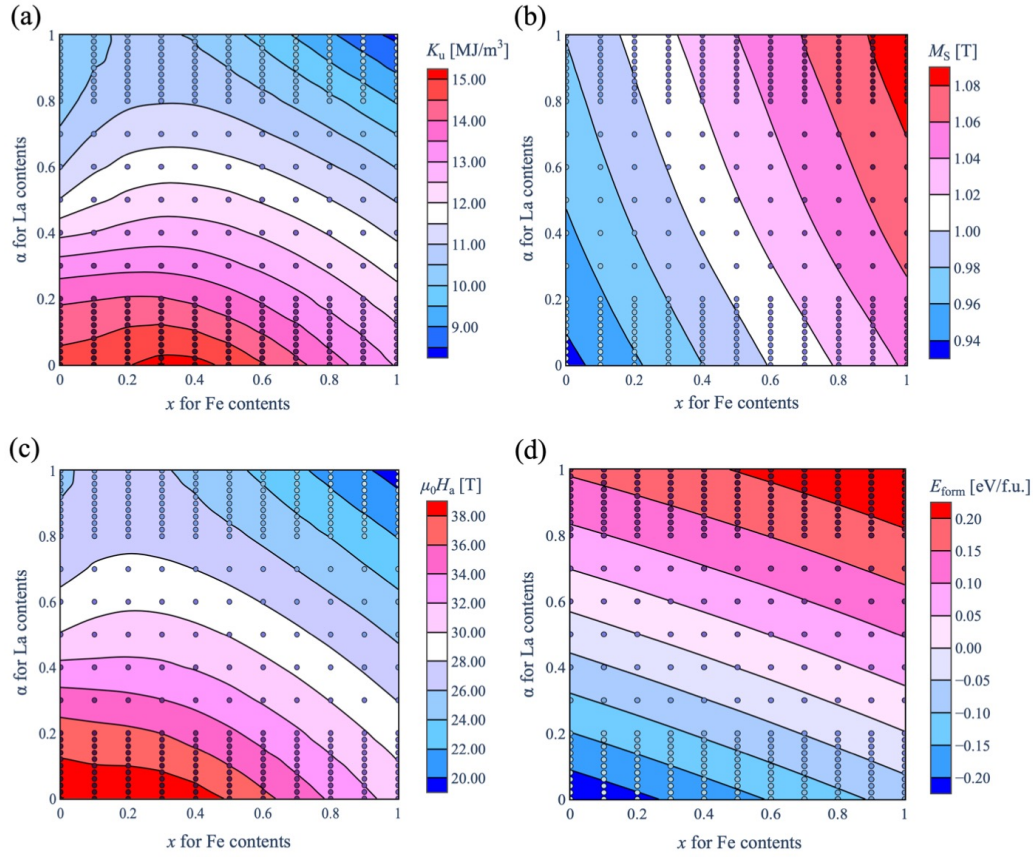
Figure 1: Calculated (a) magnetic anisotropy (K_u), (b) magnetization (M_s), (c) anisotropic field ($\mu_0 H_a$), and (d) formation energy (E_{form}) for $\mathrm{Ce_{1-\alpha}La_\alpha Co_{5-x}Fe_x}$.

the mean-field approximation. The calculated T_C of $\mathrm{CeFe_5}$ and $\mathrm{LaCo_5}$ are 1357 K and 1176 K, respectively. These values are higher than that of $\mathrm{CeCo_5}$. Our calculation confirms that both the Fe and La doping lead to the increase of T_C. In particular, $\mathrm{CeCo_{4.7}Fe_{0.3}}$ has rather higher T_C of 1005 K

References

[1] H. Okumura, T. Fukushima, H. Akai, and M. Ogura, Solid State Commun. **373-374**, 115257 (2023).

First-principles study of magnetic materials

Takashi MIYAKE

CD-FMat, National Institute of Advanced Industrial Science and Technology
Umezono, Tsukuba, Ibaraki 305-8568

We have performed systematic first-principles calculations of transition metal compounds for the development of magnetic materials. This year, we focused on iron-cobalt systems. Calculations were performed by changing the composition of iron and cobalt and the lattice constants.

The calculation is based on density functional theory in the local density approximation. We use AkaiKKR which is based on the Korringa-Kohn-Rostoker Green function method. Chemical disorder is treated within the coherent potential approximation (CPA) which is the best single-site approximation for disordered alloys.

Figure 1 shows the magnetic moment of Fe-Co systems for (a) Fe, (b) $Fe_{0.8}Co_{0.2}$, (c) $Fe_{0.6}Co_{0.4}$, (d) $Fe_{0.4}Co_{0.6}$, (e) $Fe_{0.2}Co_{0.8}$, and (f) Co. The horizontal line is c/a, where $c/a=1$ means the bcc structure, and $c/a = \sqrt{2}$ is the fcc structure. Starting from iron in the bcc structure and increasing c/a, the magnetic moment decreases. Starting from iron in the bcc structure and increasing the cobalt concentration, the magnetic moment increases then turns to decrease, as is well-known in the Slater-Pauling curve. The calculations of the Curie temperature and other transition-metal alloys are now underway.

We have also carried out systematic first-principles calculation of $A_{2-x}B_xMo_3N$ in the β-Mn phase by changing A and B elements (Fig. 2). The magnetic moment is calculated, and chemical composition having high magnetic moment is proposed.
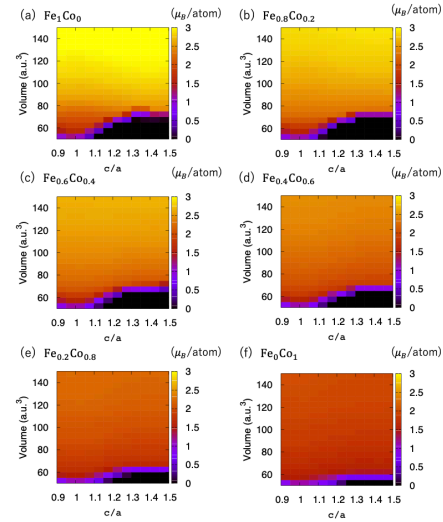

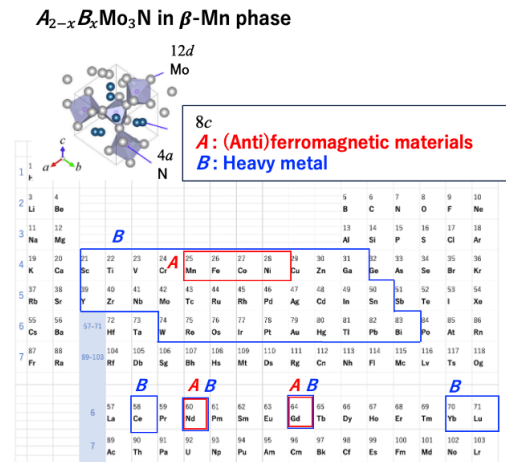Figure 1: Magnetic moment of Fe-Co systems.

Figure 2: First-principles calculation of $A_{2-x}B_xMo_3N$ in the β-Mn phase.

Construction of NNP for Fe-Ti-N

Junping Du and Shigenobu Ogata

Department of Mechanical Science and Bioengineering,

Osaka University 1-3 Machikaneyama-cho, Toyonaka, Osaka 560-8531, Japan

We have trained a neural network potential (NNP) for the Fe-Ti-N system using the Deepkit framework [1,2]. The density functional theory (DFT) calculations were conducted to prepare the training dataset using the VASP software. The training dataset contains the designed atomic models with monoatomic, binary, and ternary elements, which were obtained using the supercomputer system "Ohtaka" at the ISSP.

Because of the low concentration of Ti and N (~1%) in the Fe-Ti-N system we studied, the matrix properties of the system are represented by the BCC-Fe. Therefore, we designed a BCC-Fe supercell model with 54 atoms. Various deformations were applied to this model and various configurations were sampled by direct molecular dynamics simulations at 0~1000 K using a NNP of Fe [3]. The configurations of vacancy, the surfaces, the γ surface, and the two-dimensional Peierls potential of the screw dislocation, were also designed. The results of the DFT calculations for these configurations constitute the BCC-Fe dataset.

Considering that B1-TiN is the precipitated phase in this system, we have taken the information on the B1-TiN phase as an important part of the dataset. We constructed a 108-atom model of B1-TiN, applied different deformations to this model as well, and conducted FPMD simulations using VASP at 200 K~1000 K, thus giving the dataset of TiN.

Since the property of the Fe/TiN interface controls the TiN precipitation process, we also designed a dataset of this interfacial system. The various configurations of Ti and N in BCC-Fe forming a solid solution were also designed to model the precipitation process.

Based on the above DFT dataset, which contains 23,866 configurations, the Fe-Ti-N NNP was successfully trained using the Deepkit framework, and root-mean-squared errors of the energy and the force are 3 meV and 12 meV/Å. For the training of NNP based on Deepkit framework, "Kugui" accelerator server was used.

References

[1] H. Wang, L. Zhang, J. Han, and W. E. **Comput. Phys. Commun. 228**, 178 (2018).

[2] J. Zeng, D. Zhang, D. Lu, P. Mo, Z. Li, Y. Chen, M. Rynik, L.A. Huang, Z. Li, S. Shi, Y. Wang, et al. **J. Chem. Phys. 159**, 054801 (2023).

[3] F.S. Meng, J.P. Du, S. Shinzato, H. Mori, P. Yu, K. Matsubara, N. Ishikawa, and S. Ogata, **Phys. Rev. Mater. 11**, 113606 (2021)

Exploration of Ferroelectric Materials using Large-scale Computations

Kazuki SHITARA

Nanostructures Research Laboratory,

Japan Fine Ceramics Center, 2-4-1 Mutsuno, Nagoya, Aichi 456-858

Recently, ferroelectricity has been reported in crystal structures other than the perovskite structure such as the wurtzite and fluorite structures. For example, ferroelectricity has been experimentally observed in AlN and ZnO which have the wurtzite structures[1]. Theoretical calculations play an important role in understanding the mechanism of ferroelectricity in such new crystal structures. In this study, we performed comprehensive first-principles calculations to obtain the guidelines for designing ferroelectric materials.

Figure 1 shows SHAP analysis results to explore the dominant factors on the energy barrier of polarization reversal. It shows the extent to which each descriptor affects the energy barrier, and provides guidance on adjusting the descriptor's value to increase or decrease the barrier energy. For example, we found that reducing the sum of boiling points of simple substances results in a smaller energy barrier. This corresponds to the fact that the boiling points of Si, C, and B, which are highly covalent, and their formal charges are high.

We applied a similar analysis to spontaneous polarization. By extracting dominant factors from a wide composition range, a reciprocal relationship is found between the spontaneous polarization and the energy barrier, which is controlled by the valence of cation and anion. Simultaneously, it is suggested that the energy barrier can be reduced while maintaining a high spontaneous polarization value by controlling ionic/covalent bonding, thereby proposing specific material design guidelines to break away from the reciprocal relationship.

References

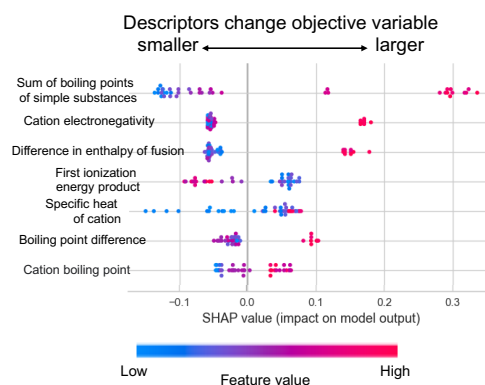[1] K. Ferri, *et al.*, J. Appl. Phys. **130** (2021).

Fig. 1: Results of dominant factor analysis using machine learning (SHAP analysis)

Systematic evaluation of solubility of polypeptides in solvents by free energy calculation method using all-atom model

Kazuo YAMADA and Nobuyuki MATUBAYASI

Division of Chemical Engineering, Graduate School of Engineering Science,

Osaka University, Toyonaka, Osaka 560-8531

The development of biopharmaceuticals using polypeptides, which are artificially synthesized using proteinogenic amino acids as building blocks, is anticipated in the field of pharmaceuticals. This is due to the fact that artificial polypeptides possess the advantageous property of biodegradability, whereas conventional, PEG-modified ones are often not biodegradable. Natural peptides are composed of 20 kinds of amino acids, including glycine (Gly), alanine (Ala), serine (Ser), aspartic acid (Asp), lysine (Lys), and arginine (Arg), among others. These amino acids can be combined in various ways to synthesize a vast array of artificial polypeptides. Solubility and partition coefficient in in vivo solvent environments, such as water and saline solutions, are crucial physical quantities for controlling pharmacokinetics, including absorption, distribution, metabolism, and excretion. Therefore, it is imperative to systematically explore the solubility and partition coefficient in water in connection to amino acid sequences. Given the vast number of possible amino acid sequences, computer simulation is an invaluable tool for evaluating the solubilities of peptides in water.

To analyze the solubilities at atomic resolution, we employ all-atom molecular dynamics (MD) simulation. We focus on homo-tetrapeptides as model systems and identify the intermolecular interaction components that are responsible for the solubilities. The key is the free-energy calculation. By combining MD simulation and the energy-representation theory of solvation [1,2], we obtain the free energies determining the solubilities. The solubility of a peptide molecule is determined as the difference of its solvation free energy in water from the free energy of insertion of a single molecule of the peptide into the pure solid. The insertion free energy into the solid can also be treated as a solvation free energy by viewing the inserted peptide as the solute and the other peptide molecules as the solvent. We extend the energy-representation method of solvation to the solid systems in this work.

The free energies of solvation were calculated for 15, different homo-tetrapeptides in the single-component pure solid systems and in the aqueous solutions at infinite dilution. The equilibration and sampling calculations were

performed using GROMACS 2016.4 [1], while the solvation free energies were computed using ERmod [2]. MD simulation with GROMACS were performed in parallel using GPU nodes, and ERmod was on CPU nodes.
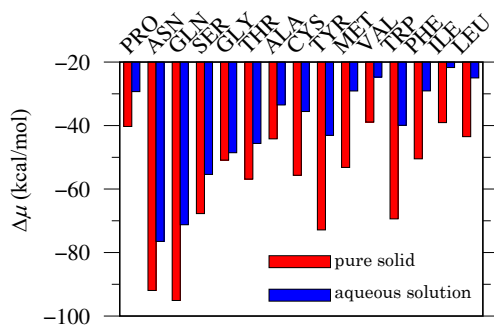

Fig. 1: Free energies of solvation $\Delta\mu$ of homo-tetrapeptides in their pure solids and aqueous solutions; the differences between the two solvation free energies provide the water solubilities of the peptides.

Figure 1 shows the free energies of solvation $\Delta\mu$ of 15 tetrapeptides. The experimentally measured solubility of a single amino acid in water is lower and more hydrophobic from left to right. Since the dissolution refers to the transfer of a peptide molecule from its solid to the aqueous solution, the solubility is given by the difference in $\Delta\mu$ between the solid and aqueous solution. It is then seen in Figure 1 that the peptide dependence of $\Delta\mu$ is parallel between the solid and aqueous solution. This means that the solubility cannot be ranked simply by the affinity of the peptide to water.

The solvation free energies were further decomposed to identify the intermolecular-interaction components determining the dependence of the solubilities into water on the peptide species. The excluded-volume component exhibited the strongest correlation with the peptide solubility of peptide, with a correlation coefficient of 0.86. The excluded-volume component is the free-energy penalty required for displacing solvent molecules from the region to which the solute molecule is to be inserted. A negative correlation was observed, with a coefficient of –0.13, for the direct interaction energy between the solute, peptide molecule and the solvent molecules against the solubility of the peptide into water. The above results indicate that the excluded-volume component is a more important factor for the solubility into water than the direct interaction energy such as the hydrogen bonding.

The effect of added salt on the solubility of model compounds were also addressed through free-energy decomposition [3]. In this case, too, the importance of the excluded-volume effect was pointed out.

References

[1] M. J. Abraham, *et. al*, SoftwareX **1-2** (2015) 19–25

[2] S. Sakuraba and N. Matubayasi: J. Comput. Chem. **35** (2014) 1592-1608

[3] S. Hervø-Hansen, D. Lin, K. Kasahara, and N. Matubayasi: Chem. Sci. **15** (2024) 477-489

First-principles study toward elucidating the proton transfer mechanism with nuclear quantum effect

Tomomi Shimazaki

Graduate School of Nanobioscience,

Yokohama City University, 22-2 Seto, Kanazawa, Yokohama 236-0027

The quantum nature of nuclei can affect various physical and chemical properties on atomic-scale systems. Especially, the proton is the lightest element, and hence it is important to deal with nuclear quantum effects to study its behavior in detail. In this study, we investigate the proton transfer mechanism in water using the first-principles path integral (PIMD) method. For comparison, we also performed simulations for D+ in heavy water (D_2O) as well as H+ in light water (H_2O). As a result, it was observed that H_3O+ tends to have a trigonal pyramidal structure in the solvent, while D_3O+ is more likely to have a planar structure, which may be due to the difference in the oxygen-oxygen structure in the first and second hydration spheres, as seen in **Fig. 1**.

However, the first-principles PIMD method is computationally expensive and difficult to apply to large-scale models. Therefore, we tried to develop the QM/MM method. For the MM program, we employed MODYLAS, which has been used in many large-scale simulations on Fugaku. We modified the source code of MODYLAS and implemented an interface with a QM program.

On the other hand, even if the QM/MM method is used, the computational cost of the QM part is very high for large-scale simulations. Therefore, we attempted to build a prediction model for QM calculations using a machine learning (neural network) model. We confirmed that the machine learning (ML) model can give good prediction performance for test systems.[1] In the next step, we will perform QM/ML/MM simulations by incorporating the machine learning model (ML) into the QM/MM method.
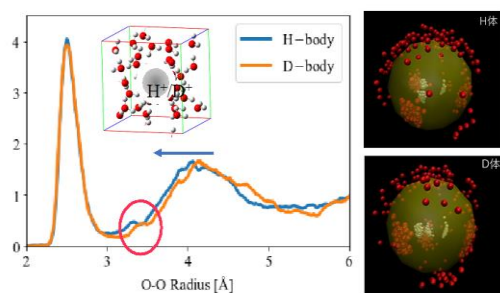

Fig 1. The structure around the proton obtained by first-principles simulation including nuclear quantum effects.

[1] Tomommi Shimazaki and Masanori Tachikawa, Chem. Phys. Lett, 829, 140744, 2023.

Phonon-calculation method for magnetic random alloys

Y. Gohda[1], T. Tadano[2], T. Miyake[3], and T. Ohkubo[2]

[1]*Dept. Mater. Sci. Eng., Tokyo Tech, Yokohama 226-8502, Japan*
[2]*DXMag, National Institute for Materials Science, Tsukuba 305-0047, Japan*
[3]*CD-FMat, AIST, Tsukuba 305-8658, Japan*

Phase equilibria can be discussed from phase diagrams that are constructed from free energies of multiple phases. First-principles phonon calculations play a significant roles in evaluating free energies. Since phonon dispersions of random alloys are broadened, band unfolding techniques are necessary as same as electronic band structures.

In this project, we developed a band-unfolding method within first-principles phonon calculations using the direct method. In the original Brillouin zone of the supercell, many important details of the band structure are hidden in the spaghetti bands resulting from different modes of numerous atoms within the supercell. By unfolding the band, hidden band gaps are revealed, and it becomes easier to make qualitative comparison between different systems based on the same primitive material. The unfolding technique is implemented into the ALAMODE code [1]. In the present study, it is made possible to incorporate impurity atoms at interstitial sites. Figure 1 shows calculated band dispersions of Ti-Al alloys without and with oxygen interstitials. Ti-Al is in the ordered α_2 phase with the $D0_{19}$ structure. However, since the

alloy is off-stoichiometric (stoichiometric: Ti_3Al), phonon bands become broadened even in the binary form. It is clear from the figure that interstitial oxygen makes phonon dispersion broadened further. The present method is applicable for magnetic materials, where the difference in the spin directions causes broadning of phonon dispersions. In addition, phase equilibria in permanent magnets were discussed through the CALPHAD approach with the first-principles cluster-expansion method [2].
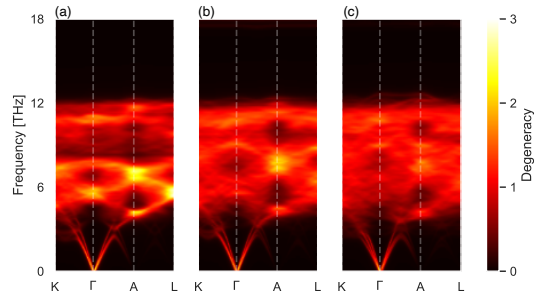

Figure 1: Changes in the effective phonon-band structure for Ti-Al alloys (at.37.5% of Al) in the α_2 phase with the $D0_{19}$ structure in (a) a binary form and with (b) 2 and (c) 5 interstitial O atoms within 64-site supercell.

[1] T. Tadano, Y. Gohda, and S. Tsuneyuki, J. Phys.: Condens. Matter **26**, 225402 (2014).
[2] S. Enomoto, S. Kou, T. Abe, and Y. Gohda, J. Alloys Compd. **950**, 169849 (2023).